A Micromechanics Approach for Polymeric Material Failures in Microelectronic Packaging

X.J. Fan[1], G.Q. Zhang[2], L. J. Ernst[3]
[1)] Philips Research USA, 345 Scarborough Road, Briarcliff Manor, NY 10510, USA
Tel: 914-945-6338, Fax: 914-945-6014, email: xuejun.fan@philips.com
[2)] Philips-CFT, P.O. Box 218, 5600 MD Eindhoven, The Netherlands
Tel: +31402733825, Fax: 31-40-2735996, g.q.zhang@philips.com
[3)] Delft University of Technology, Mekelweg 2, 2628 CD Delft, The Netherlands
Tel: +31152786519, Fax: +31152782150, l.j.ernst@wbmt.tudelft.nl

Abstract

This paper presents a micromechanics-based approach to investigate the moisture-induced interface delamination of polymer materials at soldering reflow in electronic packages. We start from a model study on vapor pressure based on a micro-void approach. Then the works of single void behaviors subjected to thermal and internal vapor pressure are introduced. The focus is on the *unstable* void-growth when the finite-deformation is considered. Detailed discussions are given to illustrate why the current models do not explain well the phenomenon observed in actual packages. Since the interface delamination is considered as consequences of the void growth, nucleation and coalescence, the Gurson's model is introduced to link the microscopic single void behaviors to the macroscopic continuum descriptions. It shows that the developed vapor pressure model provides the evolution equation for the vapor pressure as one of additional internal variables for the modified Guron's model. Finally a discussion is given on the moisture-induced failure mechanism analysis. It is emphasized that the moisture-induced interface delamination not only depends on the vapor pressure, but also on the interface strength as function of moisture as well.

1. Introduction

Polymer materials have wide applications in microelectronic packaging. Some polymer materials are used in bulk form such as encapsulant (mold compound), carrier or printed circuit board (FR4 and BT). Some polymer materials are used as adhesives such as die-attach, underfill, or other structural and thermal adhesives. Polymers are also used in thin- or thick- film as isolation layer such as solder mask on printed circuit board or polyamide and BIB in wafer level.

Despite the diversities of the chemistry and the compositions, the polymer materials applied in microelectronics can be either thermoset or thermoplastic materials [1]. Both types of materials have glass transition temperature, above which, the material properties such as CTE and Young's modulus are very sensitive to temperature.

Another common feature of polymer materials is the high porosity, which makes the material susceptible to the moisture absorption. Let's estimate how much moisture a polymer material could absorb. Consider a typical mold compound in 85°C/85RH ambient moisture condition. A typical value of the saturated moisture concentration, denoted as C_{sat} , is $1.25e^{-2}$ g/cm^3 [2], The physical meaning of the C_{sat} is the moisture density over the *total* material volume. A comparison can be made for the C_{sat} to the ambient moisture (vapor) density at 85°C/85RH, i.e., $\rho_{ext}=0.85\rho_g=3.04e^{-4}$ g/cm^3, where ρ_g is the saturated vapor density at 85°C. It is straightforward to note that $C_{sat}=41\rho_{ext}$! This implies that the most amount of moisture in material must be condensed into the liquid form. The moisture absorbed by material is in the mixed liquid/vapor phase. In fact, the diffusion process of moisture is the transport process of moisture from ambient to material inside by moisture condensation. The moisture will stay in micro-pores or free spaces in material.

The moisture-induced failure is a unique problem, which occurs only in electronic packaging field other than other engineering fields. The moisture contributes to the failures mainly from two aspects. One is the evaporation of the moisture during temperature rise, generating high internal vapor pressure, and the other, is the reduction of the interface strength with the moisture absorption. The combination of these two effects makes this problem prominent and severe during the surface mounting of electronic packages onto the printed circuit board.

The moisture-induced failure undergoes four different stages, which are schematically depicted in Fig. 1 [3]. In stage 1 (preconditioning), the package absorbs moisture from the environment, which condenses in micropores in polymer materials such as substrate, die attach, mold compound and along the interfaces. Preconditioning is a time-consuming process, and usually takes a few days or even months in controlled or un-controlled humid environment. In stage 2, the package is mounted to the printed circuit board by soldering. The entire package is exposed to temperatures as high as 220°C. As a result, the condensed moisture vaporizes under high temperature associated with the soldering process. The vapor pressure and the reduction of the interface strength at high temperature due to the moisture intake will cause small interfacial delamination. In stage 3, the vapor pressure exerts traction loading on the delamination area, eventually causing the package bulge. In the final stage, the package crack forms and propagates laterally outwards. When the crack reaches the package exterior, the high-vapor pressure water vapor is suddenly released, producing an audible sound like popcorning.

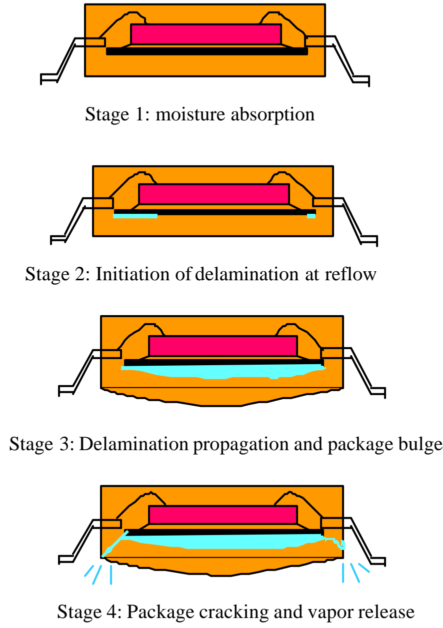

Fig.1 Schematic of four stages of the moisture-induced failures in a plastic electronic package. Stage 1 is a time-consuming process, which takes a few days or even months in a controlled or un-controlled humid enviroment. Stage 2 occurs at soldering reflow temperature around 220°C. It takes a few minutes to heat up the package in stage 2.

Traditional approach to deal with the delamination uses linear or nonlinear interface fracture mechanics, by which the failure is represented by a global parameter such as energy release rate, without the incorporation of microscopic aspects of the rupture process[4,5,6,7]. By this approach, a pre-existing macroscopic crack prior to the reflow soldering is assumed. And the vapor pressure is taken as traction loading on the delaminated crack surfaces. Such an analysis is very helpful to understand the package behaviors in stages 3 and 4 during reflow to prevent the delamination propagation and package cracking, but provides little insights on the failure-mechanism for the initiation of delamination. The process for stages 3 and 4 is usually very rapid and difficult to control once there is a small delamination initiated along the interface.

Therefore, it is critical to understand the failure mechanism in stage 2, i.e., the initiation of the delamination. Two key issues are associated with the delamination formation. One is the modeling of vapor pressure evolution as function of moisture, void size and temperature rise. The other, the dependency of the interface strength as function of temperature and moisture. The void growth, nucleation and the subsequent coalescence have been long recognized as the ultimate failure mechanism of the interface delamination for the moisture-induced failure [8,9]. Therefore, a micro-mechanics-based approach is introduced to investigate the problem.

In this paper, a vapor pressure model is introduced first based on a micro-void approach[3,10,11,12]. The key features associated with this model are highlighted. This model is extended to consider the effects of thermal expansion and void growth. Next the works of the unstable growth of a single-void subjected to the vapor pressure and thermal loading [13,14] is introduced and applied to analyze the void behaviors in a humid enviromental condition. Then a continuum description with consideration of the internal vapor pressure as an additional variable is introduced by using the Gurson model [15]. The concept of cell model [16]and its application[17] in electronic packaging is briefed. Finally, the mechanism analysis for the moisture-induced delamination is discussed.

2. Vapor Pressure Modeling: a Micro-Void Approach

Previous studies assume that the moisture is always in a single vapor phase throughout the temperature rise[8], and hence the ideal gas law can be applied for the evolution of the internal vapor pressure inside voids. Since such a vapor pressure model is not linked to the moisture property of the material, it is difficult to estimate the initial or reference vapor presure at reference temperature (e.g. temperature T_0 at precoditioning). The problem becomes very complicated when the moisture in voids is at mixed liquid/vapor phase, which occurs in most of cases for polymer materials.

One of critical issues in developing a vapor pressure model is to find out the moisture density in *voids*, denoted as ρ. As we know, the moisture concentration C, the moisture density over *bulk* volume, can be easily obtained from the moisture diffusion analysis at preconditioning. The relation between ρ and C can then be established by the introduction of the *void volume fraction f*, as following[3],

$$\rho = \frac{\mathrm{d}m}{\mathrm{d}V_f} = \frac{\mathrm{d}m}{\mathrm{d}V}\frac{\mathrm{d}V}{\mathrm{d}V_f} = C/f \qquad (1)$$

where $\mathrm{d}m$ is the moisture mass over bulk volume $\mathrm{d}V$ (representative volume element, RVE)[3], $\mathrm{d}V_f$ is the total void volume over $\mathrm{d}V$, and f is the void volume fraction defined as $\mathrm{d}V_f/\mathrm{d}V$. Thus $0<f\leq 1$. It is of main interests to investigate the evolution of the void volume fraction f in micromechanics analysis (which will be discussed in subsequent sections). f = 1 refers the formation of the delamination in macroscopic sense, in which the RVE is totally voided.

As discussed before, the saturated moisture concentration $C_{sat}=41\rho_{ext}$ at 85°C/85RH condition for a typical mold compound. Assume that the void volume fraction f is 0.05, equation (1) gives $\rho=820\rho_{ext}$. This numbers clearly shows that how much moisture a typical polymer material could absorb. Such an amount of moisture must condense into the mixed liquid/vapor phase in material. However, if less moisture is taken, the moisture may still be in single vapor phase. The following condition is used to determine the moisture state in voids at preconditioning of temperature T_0,

$$\begin{cases} \rho \leq \rho_g(T_0) & \text{for vapor phase at } T_0 \\ \rho > \rho_g(T_0) & \text{for mixed liquid/vapor phase at } T_0 \end{cases} \qquad (2)$$

where ρ_g is the saturated vapor density, which can be obtained from the steam table as function of temperature.

When the moisture is at mixed liquid/vapor phase, it is necessary to know at which temperature the moisture can be *fully* vaporized. This temperature is called the *phase transition temperature*, denoted by T_1, which can be determined by

$$\rho(T_1) = \rho_g(T_1) \tag{3}$$

Now the vapor pressure in voids can be determined by the moisture state analyzed above. When the moisture is in the mixed liquid/vapor phase, the vapor pressure maintains the saturated vapor pressure p_g as function of temperature (from steam table), i.e.,

$$p(T) = p_g(T) \quad \text{for mixed liquid/vapor phase} \tag{4}$$

When the moisture is in single vapor phase, the ideal gas law can be followed to calculate the vapor pressure as following,

$$p\mathrm{d}V_f = \mathrm{d}mRT \tag{5}$$

or, dividing both sides by $\mathrm{d}V$

$$pf = CRT \tag{6}$$

where R is the universal gas constant (=8.314J/mol).

The two states (p, f, T, C) and (p_0, f_0, T_0, C_0) are then related by

$$\frac{p}{p_0} = \frac{Tf_0C}{T_0 fC_0} \quad \text{for single vapor phase from } T_0 \text{ to } T \tag{7}$$

where p_0 is related to the local moisture concentration at T_0, as analyzed in ref. [10].

A complete vapor pressure model with three distinct cases has been developed in ref. [10] based on the above analysis. Finite element modeling on the whole field vapor pressure distribution over the entire package is proceeded after the moisture diffusion modeling [11]. The desorption effect is also taken into considerations. The model, however, does not consider the void growth and the thermal expansion effect.

Assume that the material is incompressible, the change of volume element due to the temperature change and the void volume fraction change are related by[13]

$$\frac{dV}{dV_0} = \frac{1-f_0}{1-f} e^{3\alpha\Delta T} \tag{8}$$

where $\Delta T = T - T_0$. Thus

$$C = \frac{\mathrm{d}m}{\mathrm{d}V} = \frac{\mathrm{d}m}{\mathrm{d}V_0}\frac{\mathrm{d}V_0}{\mathrm{d}V} = C_0 \frac{1-f}{1-f_0} e^{-3\alpha\Delta T} \tag{9}$$

in which C_0 and $\mathrm{d}V_0$ are the moisture concentration, and the RVE volume at preconditioning T_0, respectively. $\mathrm{d}V$ is the cell volume at current temperature T. It should be noted that although the moisture mass is assumed conserved during the temperature rise (the desorption effect is neglected), the moisture concentration may change due to the change of the bulk volume.

Given the initial moisture concentration C_0 (from moisture diffusion analysis), the initial void volume fraction f_0 , and the current void volume fraction f , the vapor pressure at current temperature T can then be determined by

Case 1: when $C_0 / f_0 \le \rho_g(T_0)$,

$$p(T) = \frac{C_0 p_g(T_0)}{\rho_g(T_0) f} \frac{T}{T_0} \frac{1-f}{1-f_0} e^{-3\alpha(T-T_0)} \tag{10}$$

Case 2: when $\frac{C_0}{f}\frac{1-f}{1-f_0} e^{-3\alpha(T-T_0)} \ge \rho_g(T)$

$$p(T) = p_g(T) \tag{11}$$

Case 3: when $C_0 / f_0 > \rho_g(T_0)$, and

$$\frac{C_0}{f}\frac{1-f}{1-f_0} e^{-3\alpha(T-T_0)} < \rho_g(T)$$

$$p(T) = p_g(T_1) \frac{T}{T_1} \frac{f(T_1)}{f} \frac{1-f}{1-f(T_1)} e^{-3\alpha(T-T_1)} \tag{12}$$

where T_1 is determined by

$$\frac{C_0}{f(T_1)} \frac{1-f(T_1)}{1-f_0} e^{-3\alpha(T-T_1)} = \rho_g(T_1) \tag{13}$$

The three cases can be schematically depicted in Fig. 2. The above model includes an unknown f, the current void volume fraction. Obviously, the vapor pressure is dependent on the void deformation behaviors, and should be solved together with the governing equations of deformation. It is noted that *total* RVE volume given by equation (8) is obtained from a finite single void

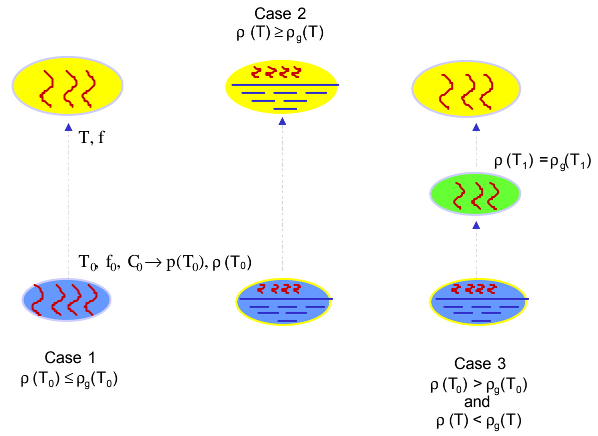

Fig.2 Three distinct cases for the vapor pressure evolution from preconditioning temperature T_0 to the desired temperature T. In case 1, the moisture in void is in single vapor phase at T_0, thus the vapor pressure at T follows the ideal gas law. In case 2, the moisture in void is in the mixed liquid/vapor phase at *temperature T* (must be mixed liquid/vapor phase at T_0 too), thus the vapor pressure maintains the saturated vapor pressure during the course of temperature rise. Case 3 is in between case 1 and case 2, where the moisture in the mixed liquid/vapor phase at T_0, but single vapor phase at T. The phase transition temperature T_1 where the moisture is just *fully* vaporized should be determined first. Then vapor pressure at T follows ideal gas law from T_1. The complete equations are given in equations (10)-(13).

solution[13]. With $f \to 1$, equation (8) gives $dV/dV_0 \to \infty$. It is true for a single void due to the volume incompressibility. However, a RVE always has a finite volume, even when $f \to 1$. Besides, the moisture density defined by equation (1) is linked to the *physical* volume of the voids in a RVE. Therefore, in using the evolution equation of vapor pressure in Gurson's model (which will be discussed in section 4), the above equations should be modified, which are given in Appendix.

Let's investigate the magnitude of vapor pressure for case 1, where the moisture is fully vaporized at preconditioning. Assuming that the preconditioning temperature T_0 is 85°C, the *maximum* vapor pressure allowed in voids at T_0 is then the saturated vapor pressure $p_g(T_0=85°C) = 5.27e\text{-}2$ MPa. The vapor pressure at reflow temperature $T= 220°C$ is plotted as function of the current void volume fraction f in Fig. 3, by using equation (10) (α=200ppm/°C, f_0=0.03). The vapor pressure decreases with the current void volume fraction. The pressure may be lower than the initial vapor pressure of T_0 when the void becomes large. The maximum vapor pressure developed at 220°C is 7.92e-2 MPa, when the void does not grow ($f=f_0$). This implies that the vapor pressure for *case 1* is extremely low that it has almost negligible effect on the void growth.

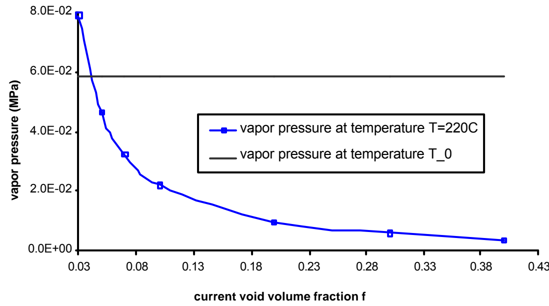

Fig.3 Vapor pressure p at 220°C versus the current void volume fraction f by equation (10) for case 1, with f_0=0.03, α=200ppm/°C, T_0=85°C, and $p_0 = p_{0max} = p_g(85°C) = 5.27e\text{-}2$ MPa. It shows that the vapor pressure for *case 1* is extremely low and has almost negligible effect on the void growth.

Consider the case 2 where the moisture is not fully vaporized at reflow temperature T. In this case the vapor pressure is the saturated vapor pressure, i.e., $p=p_g(T=220°C)=2.32$ MPa . The vapor pressure with such a magnitude will have significant effect on the void behavior, which will be discussed in subsequent sections.

Questions remain that how to measure the initial void volume fraction f_0. An approximate method in estimating the initial void volume fraction is proposed in refs. [3,10,11] by using the moisture absorption test. From equation (1), when moisture absorption is saturated, the initial void volume fraction is given by

$$f_0 = \frac{C_{sat}}{\rho} \tag{14}$$

Given the fact that the moisture condenses mostly into the liquid form and the water liquid density is 1.0 g/cm^3, f_0 can be estimated from

$$f_0 \approx C_{sat}\big|_{100°C/100RH} \tag{15}$$

Equation (15) provides a simple way to predict the approximate magnitude of the voids fraction existing in polymer materials using the moisture property data. Ref. [10] shows that the initial void volume fraction is usually between 0.01 and 0.05.

3. Single Void Behaviors: Unstable Growth Subjected to Thermal Stress and Internal Vapor Pressure

The interface delamination is considered as the consequences of the micro-voids growth, nucleation and coalescence. Therefore, it is important to understand the deformation behaviors in micro-void level first. A micromechanics analysis of a single void is very useful to reveal some salient features and fundamental failure mechanisms associated with the initiation of the interfacial delamination. The use of the single void model is also helpful to investigate the role of vapor pressure on the void behaviors.

The effect of the mean stress on the plastic growth of a void has been studied previously by many researchers[18,19,8]. An exponential dependence of void growth rate on the triaxial stress was found. However, since the void growth is finite-deformation, Huang[20] pointed out that the consideration of the finite-deformation would lead to an *unstable* void growth. This implies that the void cell will 'burst' suddenly when the applied stress reaches its critical value.

For the purpose of analysis, we consider a spherical volume of material containing a microvoid of spherical shape, as shown in Fig. 4. The material is incompressible. The inner radial surface is subjected to internal vapor pressure, induced by the moisture inside. The vapor pressure p follows the rules we discussed in section 2. A radial stress σ^T is applied to outer radius to represent the thermal stress as function of temperature rise. The radial equilibrium solution of a spherically symmetric cell in current configuration is the found to be[9,13]

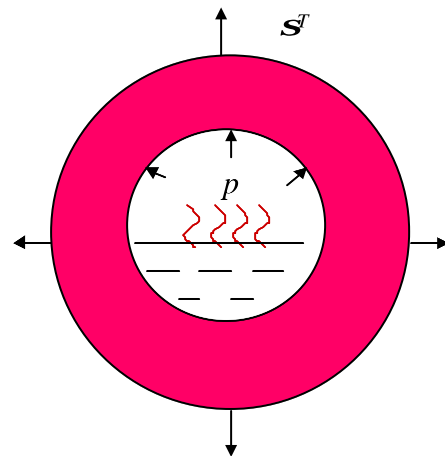

Fig.4 A micromechanics model of singe void in finite matrix in current configuration. The moisture mass is assumed conserved inside. The cell is subjected to the internal vapor pressure as well as radial thermal stress at outer radius. The deformation is finite.

$$\frac{\sigma^T(T)+p(T,f,T_0,f_0,C_0)}{\sigma_0}=\int_{\varepsilon_1}^{\varepsilon_2}\frac{H(\varepsilon)d\varepsilon}{1-\exp(-\frac{3}{2}\varepsilon)} \quad (16)$$

where ε_1 and ε_2 are the radial strains at the two-end points of the cell, which can be determined by the current and initial void volume fractions:

$$\varepsilon_1=\frac{2}{3}\ln\left(\frac{f_0}{f}\frac{1-f}{1-f_0}\right)$$
$$\varepsilon_2=\frac{2}{3}\ln\left(\frac{1-f}{1-f_0}\right) \quad (17)$$

$H(\varepsilon)$ in equation (16) denotes the true stress-logarithmic strain relation as following

$$\frac{\sigma}{\sigma_0}=H(\varepsilon)=\begin{cases}\varepsilon/\varepsilon_0 & \text{if } |\varepsilon|<\varepsilon_0\\ (|\varepsilon|/\varepsilon_0)^N\ \mathrm{sign}(\varepsilon) & \text{if } |\varepsilon|\ge\varepsilon_0\end{cases} \quad (18)$$

where σ_0 is the yield stress.

Equation (16) displays a nonlinear and non-monotonic relation between the current volume fraction f and the sum of the internal vapor pressure p and the externally imposed radial thermal stress σ^T. Fig. 5 presents the results of the void volume increase with respect to the applied traction σ^T+p, when the initial void volume fraction f_0 takes 0.01 and 0.05 respectively. The applied traction increases continuously from zero to its peak value and then decreases, which implies that the cell will collapse when the peak valued is reached. From Fig.5 it can be seen that the critical stress σ_{cr} for the unstable void growth is about 2-3 times of the yielding stress σ_0, when the initial void volume fraction is in the range 0.01-0.05.

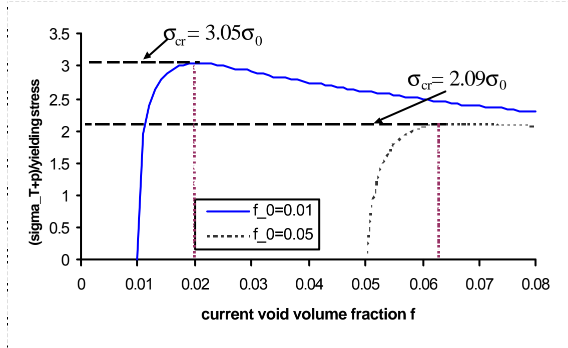

Fig. 5 The sum of thermal stress and vapor pressure applied to cavity in a finite matrix versus evolution of void volume fraction f with f_0=0.01 and 0.05 respectively (N=0.1, ε_0=0.01). It shows that the applied traction increases from zero with the void growth first. When the peak value is reached, the void growth becomes unstable. The applied loading capacity drops dramatically. The cell will 'collapse'. The critical stress for the unstable void growth is in about 2-3 times of yielding stress when the initial volume fraction is between 0.01 and 0.05.

Given the initial moisture concentration C_0, the thermal expansion (to obtain σ^T) and the initial void volume fraction f_0, euqation (16) can be solved together with the vapor equations (10)-(13) to determine the current void volume fraction as well as the vapor pressure as function of temperature. A critical temperature can then be found when the sum of applied thermal stress and vapor pressure reaches the peak value. The growth of the void cell at this temperature becomes unstable, and failure takes place.

Assume that the initial void volume fraction f_0 is 0.05, and the thermal stress can be estimated by $\sigma^T=\alpha E(T-T_{\text{stress-free}})$, in which α=200ppm/°C and $T_{\text{stress-free}}$=150°C. The critical temperature where the void unstable growth occurs is usually well above the glass transition temperature. The Young's modulus is decreased dramatically after the glass transition temperature. At reflow temperature 220°C, a typical Young's modulus may be in the range of 500MPa. Though the yielding strength at high temperature is not available to our best knowledge, an estimate can be made based on the Young's modulus by $\sigma_0=E\varepsilon_0$. Assume that ε_0=0.01, then the yield stress σ_0=5 MPa.

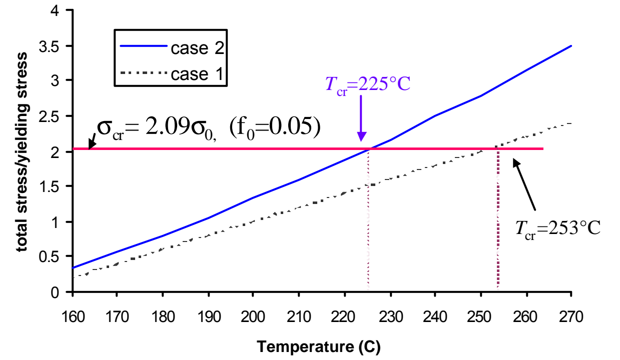

Fig. 6 The applied stress (sum of thermal strss and vapor pressure) as function of temprature rise for case 1 and 2 respectively (α=200ppm/°C, N=0.1, ε_0=0.01, f_0=0.05, E=500MPa, σ_0=5MPa). When the total stress reaches its critical stress during temperature rise, the void growth becomes unstable. The critical temperature T_{cr} for case 2 is 225°C, and 255°C for case 1. In case 1, the vapor pressure is so low that it has negligible effect on the void growth.

Let's consider the vapor pressure in two extreme cases: case 1 and case 2 (case 3 is in between case 1 and 2 as illustarted in section 2). The vapor pressure in case 1 is extremely low from the analysis in section 2 (see Fig.3), thus on calculating the left-hand side of equation (16), the vapor pressure can be neglected. For the case 2, the vapor pressure maintains the saturated state throughout the course of temperature rise. It is noted that the saturated vapor pressure increases with the temperature rise significantly. In Fig.6, the applied stress is plotted as function of temperature rise for a void with vapor pressure of case 1 and 2, repspectively. The void-growth becomes unstable when temperature reaches 225°C for the case 2. However, in case 1 where the vapor is almost negligible, the failure takes plces at a temperature as high as 255°C, well above the soldering temperature when happen at 220°C.

As we may recall, the saturated vapor pressure at 220°C is 2.32MPa. The critcal stress σ_{cr} is about 2-3 times of σ_0 (see Fig.5), i.e., σ_{cr} = 10 –15MPa, when the

initial void volume fraction is in the range 0.01-0.05. It shows that the vapor pressure takes a significant portion over the critical stress. When the lead-free solder material is used, the reflow temperature can be as high as 260-270 °C. Therefore, the saturated vapor pressure can reach 5.51MPa. Besides, the yield stress σ_0 can be even lower. The impact of the vapor pressure on the void unstable behaviors will become even more significant.

Although the predicted critical stress from the elastic-plastic model shows the important role of the vapor pressure on void deformation, the model is not able to make differences for the void behaviors at interface and in bulk. As we know, the unstable void growth is present at interfaces only during the reflow. In addition, the model is not able to explain some other phenomenon associated with the moisture-induced failure as well. For example, Fig.6 tells us that the cell may collapse when the temperature is reached to the level where the thermal stress alone reaches the critical stress for a given initial void volume fraction (case 1). However, a package without moisture intake will very unlikely fails even though the package is heated up well above the reflow temperature.

Many of the polymer materials used in electronic packages are thermoset materials, which display a rubble-like state above the glass transition temperature. The stress-strain relation expressed by the equation (18) may not be appropriate for a rubber-like material. Guo and Cheng[14] introduce the neo-Hookean model to describe the deformation behaviors of the rubber-like materials. The stored energy function can be written as following

$$W = \frac{\mu}{2}(\lambda_1^2 + \lambda_2^2 + \lambda_3^2 - 3), \quad \lambda_1 \lambda_2 \lambda_3 = 1 \qquad (19)$$

where μ is the shear modulus and λ_I are the principal stretches. It can be seen that the shear modulus is the only material property introduced in this stress-strain relation. The equilibrium solution of a spherically symmetric cell in current configuration, which is similar to equation (16), can then be expressed explicitly in terms of the initial and current void volume fractions f_0 and f as following[14]

$$\frac{\sigma^T(T) + p(f_0, f, C_0, T, T_0)}{\mu} = 2\left(\frac{1-f}{1-f_0}\right)^{1/3} + \frac{1}{2}\left(\frac{f_0}{f}\frac{1-f}{1-f_0}\right)^{4/3} - 2\left(\frac{f_0}{f}\frac{1-f}{1-f_0}\right)^{1/3} - \frac{1}{2}\left(\frac{f_0}{f}\frac{1-f}{1-f_0}\right)^{4/3} \qquad (20)$$

Again, equation (20) displays a nonlinear and non-monotonic relation between the applied stress and the void volume fraction f, as shown in Fig. 7 The unstable void growth takes place when the peak value of the sum of the thermal stress and vapor pressure is reached.

It is noted that using the neo-Hookean model by equation (19), the critical stress is of the order of the shear modulus μ Assume that the shear modulus μ=E/2(1+ν)= E/3 in incompressible case, where E is the Young's modulus, μ is about 168 MPa when E=500MPa. This implies that the critical stress is of order of 168MPa. This

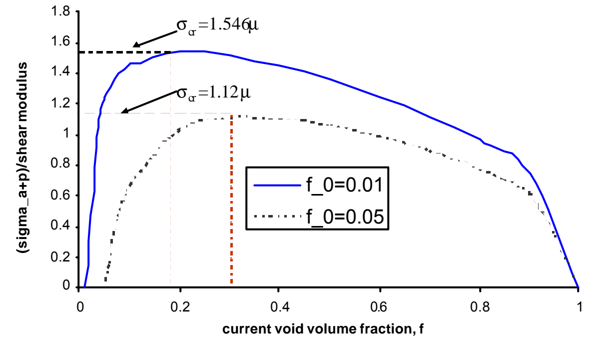

Fig. 7 The sum of thermal stress and vapor pressure applied to cavity in a finite neo-Hookean rubber-like matrix versus the evolution of void volume fraction f (f_0=0.01,and 0.05). The critical stress for the unstable void growth is of the order of the shear modulus μ when the initial void volume fraction is between 0.01and 0.05.

value is about one order higher than the predicted critical stress of 10 –15 MPa, when the elastic-plastic stress-strain relation is used. The saturated vapor pressure 2.32MPa at 220°C thus is very small compared to this critical stress 168MPa. This seems to suggest that the model study using the neo-Hookean relation does not explain well the impact of the moisture (vapor) on the material failures in reflow soldering.

On the other hands, the results obtained from the rubber-like material assumption indeed explain that the void unstable-growth can never happen in bulk material, rather than at the interfaces only. After the moisture absorption, the moisture exists anywhere in polymer materials. The moisture concentration close to the outside surface is higher that the moisture at interface if the moisture absorption is not saturated. During the soldering, the entire package is exposed to the reflow temperature at 220°C. the moisture is evaporated anywhere in material. However, the rupture of the bulk material due to the moisture prior to the interface delamination has never been observed. Failure always starts only from the interfaces with delamination. Afterwards the vapor pressure exerts traction loading on the delamination area, eventually causing the package bulge, and cracking inside bulk. This implies that even though the vapor pressure is built up anywhere in the polymer material, it has insignificant effect on the void growth in *bulk* since the portion over the critical stress is very small.

One of main reasons that the above models do not fully explain the moisture-induced failures in electronic packages is that the models are limite to homogenerous materials only. The effect of interface, in particular, the strength reduction with moisture absorption, is not accounted for. An alternative way to take the interface into consideration is to treat the interface as a special material layer that is completely different from the bulk material. This special material layer has very low Young's modulus and higher porosity. In this case the magnitude of the critical stress may be significantly reduced and the impact of the vapor pressure becomes prominent at interface layer only. However such an approach does not incorporate the interface mechanism associated with the moisture absorption. A best approach

is to incorporate the interface mechanism into the base cell model, in which the void growth is not only controlled by the applied stress, but also additionally controlled by the interface characteristic as function of moisture absorption.

4. Homogenization: Continuum Mechanics Approach Based on the Micromechanics Analysis

The micromechanics analysis based on the single-void model study, as discussed above, reveals some fundamental features associated with the failure mechanism for porous material such as the unstable growth of voids. How to link the results of single void behavior to the descriptions of material behaviors in macroscopic sense therefore becomes one of critical issues for the micromechanics analysis. This process is called homogenization process. There are several theories to establish the relationships between the microscopic and macroscopic variables[1521]. For a porous material, the void volume fraction f introduced above is treated as a *field* variable: a damage parameter to represent the local material behaviors. f=1 at a particular point implies that the delamination takes place at this 'point'. However, the void volume fraction will 'jump' to 1 from its critical value when the failure occurs, since the rupture is abrupt and unstable when f reaches the critical value.

Gurson[15] assumes that the matrix material follows the classical elastic-plastic flow rule with Von-Mises yielding criterion. He established the relationship between the macroscopic and microscopic variables by the averaging method over a cell containing a single void. Finally the macroscopic plastic potential that represents the yielding condition has the form

$$\Phi = \left(\frac{\Sigma_e}{\sigma_e}\right)^2 + 2f\cosh\left(\frac{3\Sigma_m}{2\sigma_e}\right) - (1+f^2) = 0 \tag{21}$$

in which Σ_e denotes Mises equivalent macroscopic stress, Σ_m the mean macroscopic stress, σ_e the current matrix flow strength of matrix and f the current void volume fraction. Equation (21) shows the effect of mean stress and void volume fraction on the material's yielding. Tvergaard improved the model predictions for periodic arrays of cylindrical and spherical voids by introducing two factors q_1 and q_2, as following

$$\Phi = \left(\frac{\Sigma_e}{\sigma_e}\right)^2 + 2q_1 f\cosh\left(\frac{3q_2\Sigma_m}{2\sigma_e}\right) - (1+q_1 f^2) = 0 \tag{22}$$

The Gurson yield condition was derived originally from a cell containing a traction-free void. When the internal vapor pressure is applied on void, the modified Gurson model is given by[22,13]

$$\Phi = \left(\frac{\Sigma_e}{\sigma_e}\right)^2 + 2q_1 f\cosh\left(\frac{3q_2[\Sigma_m + (1-f)p]}{2\sigma_e}\right) - (1+f^2) = 0 \tag{23}$$

It is noted that the contribution of vapor pressure to the macroscopic mean stress takes a factor form $(1-f)p$. The original Gurson-Tvergaard relation has two internal variables, σ_e and f. The extended form introduces an additional variable p. The evolution rule of the vapor pressure p obeys the equations from (A3) to (A6) and is the function of the current void volume fraction f. As discussed before, it might not be appropriate to use equations (10) to (13) for the evolution of the vapor pressure, because the vapor pressure calculation is linked to the actual physical volume of the voids. For the matrix flow stress σ_e, following evolution equation applies

$$\dot{\sigma}_e = \frac{h}{\sigma_e(1-f)}\Sigma_{ij}E^p_{ij} \tag{24}$$

where h is the hardening factor of matrix material, Σ_{ij} the macroscopic stress and E^p_{ij} the macroscopic plastic strain. For the evolution of the void growth, it includes two parts,

$$\dot{f} = \dot{f}_{growth} + \dot{f}_{nucleation} \tag{25}$$

The growth of the void is controlled by the volumetric plastic strain increment as follows (due to the incompressible condition)

$$\dot{f}_{\text{growth}} = (1-f)\dot{E}_{kk} \tag{26}$$

The increase of the void volume due to the nucleation can be given in the following form

$$\dot{f}_{nucleation} = A\dot{\sigma}_e + B\dot{\Sigma}_m \tag{27}$$

where the first term represents the matrix plastic strain-controlled nucleation and the second term, the macroscopic stress-controlled nucleation. The coefficients A and B can be determined from the normal distribution of a nucleation process.

Now the governing equations are complete for the porous material with internal variables σ_e, f and p. Given the geometry and loading conditions, the material behaviors can be simulated through the finite element implementation to investigate the local delamination process. As the voids in a particular location grow and reaches a critical size, a very rapid failure process takes place and the load carrying capacity dramatically drops. The Gurson model does not capture this coalescence phase.

The original Gurson-Tvergaard model requires each finite element to be modeled as porous material anywhere over a given structure. This usually gives rise to the difficulties in numerical implementation. Also, the model is very sensitive to the size of the element to be taken. The concept of *cell model* was thus first introduced by Xia and Shih[16] to tackle this problem. In the cell model, only a material layer of characteristic thickness D [23] is modeled by Gurson-Tvergaard relation (see Fig. 8). Beyond this region, the conventional material without voids is applied. Therefore, it can be assumed that voids are present only in the material layer from the very beginning. This model has advantage that each cell behaves as a basic material unit containing a void and can be considered as a representative volume element pertaining to the specific material considered. The discrete, three-dimensional nature of a cell enables it to capture the important features from the crack formation to

the propagation of a macro-crack. Since the Gurson-Tvergaard model is not able to capture the coalescence

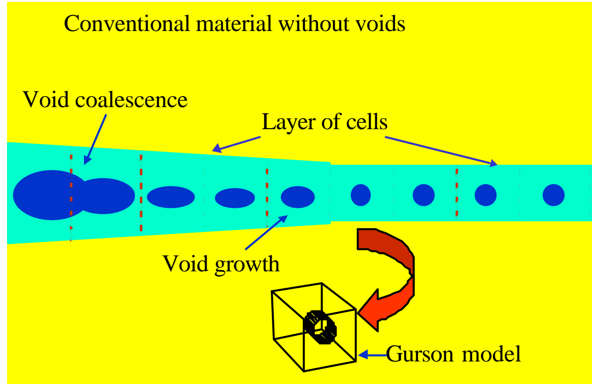

Fig. 8 Schematic of the cell model that is used to model a special material layer only such as an interface layer. The cell model uses the Gurson model before the void enters the coalescence phase. The coalescence phase is modeled by a linear traction-separation law. The cell model behaves as a basic material unit containing a void and has a characteristic thickness *D*.

phase, the cell model will use a linear traction-separation law[24] to supersede the Gurson model when the void volume fraction reaches a critical value. It should be noted that the vapor pressure model should be replaced as well by the solutions given in Appendix with f=1 from equations (A7) to (A10) when coalescence starts.

The cell model has recently been extended to model the interface delamination in plastic IC packages. The vapor pressure effect is investigated by the comparison between the baked and unbaked packages. The vapor pressure model by equation (10) for case 1 is used. However, the initial vapor pressure is assumed to be as high as 2.6 times of yielding strength. According to equation (10), the initial pressure is very small and can never exceed 5.27e-2 MPa.

One of concerns in using the Gurson-Tvergaard model is its validity for the polymer materials. Thermoset materials behave like the rubber-like at high temperatures. Thermoplastic materials behave more likely a viscous fluid or visco-elasto-plastic. Nevertheless, this mechanism-based approach provides insights into the failure of plastic packages arising from thermal and vapor pressure effects in the initiation of micro-voids, void growth, and the coalescence of voids. A specific micro-mechanics model for porous polymer materials with moisture effect is the future of the study in this field.

5. Discussions: Failure Mechanism Analysis

Moisture absorption has been long recognized as the root cause for the delamination failure at reflow. However, one of the important conclusions from the vapor pressure modeling is that the maximum vapor pressure at reflow is not always proportional to the moisture absorption. The vapor pressure maintains the saturated value (e.g. =2.32MPa at 220°C) no matter how much moisture is absorbed, as long as the moisture is not fully vaporized.

One of main missing points in above micromechanics analysis on voids growth is the interface characteristics as function of moisture absorption. In fact, the interface delamination not only depends on the vapor pressure, but also on the interface strength as well. When the vapor pressure maintains its saturated value, the interface strength becomes a key factor for the delamination. All models shown above are limited to the homogeneous materials only. Though cell model is extended to the interface problems, the moisture effect on the interface characterization is not incorporated. The effect of the moisture in above analysis is considered through the vapor pressure only.

The correlation between the interface strength and moisture absorption is very complicated. Some materials exhibit the excellent resistance to the moisture absorption, while some materials' interface strength is very sensitive to the moisture absorption. Therefore, there is no direct correlation between the amount of moisture absorbed and the failures when different materials are selected. Some failures may occur for the materials with less moisture absorption, since the adhesion of these materials is weakened significantly with moisture absorption. Some materials do not fail, even with more moisture due to the excellent resistance of interface strength against the moisture and temperature. For same materials, however, the correlation between the delamination and the moisture absorption is direct and obvious.

Therefore, it seems not appropriate to use the moisture absorption as criterion to evaluate the material's performance at reflow. The interface adhesion after moisture absorption at high temperature becomes one of most important indicators to identify the failures. The characterization and definition of the interface strength at high temperature with moisture absorption is, however, somehow ambiguous, when different methodologies and measurement techniques are applied. Nevertheless, it is noted that the interface strength at high temperature is a *comprehensive* property. Thermal stress and vapor pressure come with the temperature rise automatically and hence are the 'built-in' stresses. In other words, the interface strength measured at high temperature after preconditioning includes the effects of thermal stress and vapor pressure to a certain degree already (thermal stresses in test specimen is different from those developed in actual packages).

6. Summary

One of trends in the advanced electronic packaging development is the application of various polymeric materials for cost reduction and performance improvement. However, the susceptibility of the moisture absorption and the subsequent consequences of interface delamination at reflow temperature becomes one of major concerns for the selection of polymer materials.

A micromechancis-based approach is introduced in this paper to investigate the moisture-induced delamination. The vapor pressure modeling results from a micro-void model show that the vapor pressure is not always proportional to the amount of the moisture absorbed. The moisture in most cases will condenses into liquid/vapor mixed phase in voids and may not be fully vaporized even at reflow temperature. As a result the vapor pressure always keeps the saturated vapor pressure

at different temperature levels when the moisture is in mixed phase. This saturated vapor pressure at 220°C can be as high as 2.32MPa. The complete vapor pressure model provides the evolution process of the vapor pressure as function of moisture, void volume fraction, and the temperature.

The model study of a single-void subjected to the thermal stress and vapor pressure provides some key insights of the void behaviors. When the finite deformation is considered, the void growth becomes unstable once the applied stress reaches it critical stress, and the cell will 'burst' suddenly. Based on the single void model and the vapor pressure model, the critical temperature can be determined, at which the cell starts to collapse when the sum of the thermal stress and the vapor pressure reaches the critical stress. Since the void model is limited to the homogenous material only, it does not explain fully the failure at the interface.

The Gurson-Tvergaard model is introduced to link the microscopic variables of a single void and the macroscopic variables in continuum level. A complete continuum description is given with three internal damage variables: void volume fraction, matrix material yielding strength as well as the vapor pressure. The concept of cell model is also introduced to model a special material layer where delamination is present. The discussions are made on the validity of the Gurson's model for polymer materials.

Finally a discussion is given on the failure mechanism of moisture-induced delamination. It shows that the micromechanics approach introduced in this paper provides key insights into the failures of packages arising from the thermal and vapor pressure effects on the initiation of micro-voids. However, one of main missing points in current model studies is the lack of incorporation of the interface characteristics as function of moisture absorption. The interface delamination not only depends on the vapor pressure, but also on the interface strength as well. The interface adhesion after moisture absorption at high temperature becomes one of most important indicators to identify the failures. It is noted that the interface strength at high temperature is a *comprehensive* property. Thermal stress and vapor pressure come with the temperature rise automatically and thus are the 'built-in' stresses.

Acknowledgments

The authors are grateful for discussions with Prof. C.F. Shih, the National University of Singapore, on the cell model and its applications in the field of electronic packaging.

Appendix

Consider a representative volume element (RVE), where the void volume is $f\mathrm{d}V$. The total RVE volume change due to the temperature change is (assume that the thermal strain is small)

$$\frac{dV}{dV_0} \approx 1 + 3\boldsymbol{a}\Delta T \qquad \text{(A1)}$$

where $\Delta T = T - T_0$. Thus

$$C = \frac{\mathrm{d}m}{\mathrm{d}V} = \frac{\mathrm{d}m}{\mathrm{d}V_0}\frac{\mathrm{d}V_0}{\mathrm{d}V} = C_0(1 - 3\boldsymbol{a}\Delta T) \qquad \text{(A2)}$$

in which C_0 is the moisture concentration at preconditioning T_0. the vapor pressure at current temperature T can then be determined by

Case 1: when $C_0 / f_0 \le \boldsymbol{r}_g(T_0)$,

$$p(T) = \frac{C_0 p_g(T_0)}{\boldsymbol{r}_g(T_0) f}\frac{T}{T_0}[1 - 3\boldsymbol{a}(T - T_0)] \qquad \text{(A3)}$$

Case 2: when $\frac{C_0}{f}[1 - 3\boldsymbol{a}(T - T_0)] \ge \boldsymbol{r}_g(T)$

$$p(T) = p_g(T) \qquad \text{(A4)}$$

Case 3: when $C_0 / f_0 > \boldsymbol{r}_g(T_0)$, and

$$\frac{C_0}{f}[1 - 3\boldsymbol{a}(T - T_0)] < \boldsymbol{r}_g(T)$$

$$p(T) = p_g(T_1)\frac{T}{T_1}\frac{f(T_1)}{f}[1 - 3\boldsymbol{a}(T - T_1)] \qquad \text{(A5)}$$

where T_1 is determined by

$$\frac{C_0}{f(T_1)}[1 - 3\boldsymbol{a}(T - T_1)] = \boldsymbol{r}_g(T_1) \qquad \text{(A6)}$$

The above equations can be used to determine the vapor pressure as traction loading when delamination forms with f=1, as following

Case 1: when $C_0 / f_0 \le \boldsymbol{r}_g(T_0)$,

$$p(T) = \frac{C_0 p_g(T_0)}{\boldsymbol{r}_g(T_0)}\frac{T}{T_0}[1 - 3\boldsymbol{a}(T - T_0)] \qquad \text{(A7)}$$

Case 2: when $C_0[1 - 3\boldsymbol{a}(T - T_0)] \ge \boldsymbol{r}_g(T)$

$$p(T) = p_g(T) \qquad \text{(A8)}$$

Case 3: when $C_0 / f_0 > \boldsymbol{r}_g(T_0)$, and

$$C_0[1 - 3\boldsymbol{a}(T - T_0)] < \boldsymbol{r}_g(T)$$

$$p(T) = p_g(T_1)\frac{T}{T_1} f(T_1)[1 - 3\boldsymbol{a}(T - T_1)] \qquad \text{(A9)}$$

where T_1 is determined by

$$\frac{C_0}{f(T_1)}[1 - 3\boldsymbol{a}(T - T_1)] = \boldsymbol{r}_g(T_1) \qquad \text{(A10)}$$

References

[1] L.J.Ernst, Polymer material characterization and modeling, in Benefiting from Thermal and Mechanical Simulation in Micro-Mechanics, G.Q. Zhang et al. (eds), 2000, 37-58, Kluwer Academic Publishers

[2] J.E. Galloway and B.M. Miles, Moisture absorption and desorption predictions for plastic ball grid array packages, *IEEE Trans-CPMT-A*, 20(3), 1997, 274-279

[3] X.J. Fan & T.B. Lim, Mechanism analysis for moisture-induced failure in IC packages, *ASME International Mechanical Engineering Congress & Exposition, 11th Symposium on Mechanics of Surface Mount Technology*, IMECE/EPE-14, Nashville, Tennessee, 14-19 November, 1999

[4] A.A.O. Tay and T. Lin, Moisture diffusion and heat transfer in plastic IC packages, IEEE Trans-CPMT-A, 19(2), 1996, 186-193

[5] S Liu & Y Mei, Behaviors of delaminated plastic IC packages subjected to encapsulation cooling, moisture absorption, and wave soldering, IEEE Trans-CMPT-A, 18(3), 1995, 634-645

[6] L.T. Nguyen, K.L. Chen & J. Schaefer et al., A new criterion for package integrity under solder reflow conditions, *IEEE 45th ECTC*, 1995, 478-490

[7] M.G, Pecht, L.T. Nguyen & E.B. Hakim, *Plastic Encapsulated Microelectronics: Materials, Process, Reliability and Applications*, 1995, John Wiley & Sons

[8] X.J. Fan, S.Y. Zhang, Void behavior due to internal vapor pressure induced by temperature rise, *Journal of Materials Science*, 30, 1995, 3483-3489.

[9] Y. Huang, K.X. Hu, C.P. Yeh, N.-Y. Li & K.C. Hwang, A model study of thermal stress-induced voiding in electronic packages, *ASME Journal of Electronic Packaging*, 118, 1996, 229-234

[10] X.J.Fan, Modeling of vapor pressure during reflow for electronic packages, in *Benefiting from Thermal and Mechanical Simulation in Micro-Electronics*, G.Q. Zhang et al. (eds.), 2000, 75-92, Kluwer Academic Publishers

[11] T.Y. Tee and X.J. Fan, Modeling of whole field vapor pressure during reflow for flip chip BGA and wire-bond PBGA packages, *1st International Workshop on Electronic Materials and Packaging*, September 29-October 1, 1999, Singapore

[12] X.J.Fan, T.Y. Tee T.B. Lim, Modeling of vapor pressure during reflow for electronic packages, ASME Journal of Electronic Packaging, 1999, submitted

[13] T.F. Guo & L. Cheng, Thermal and vapor pressure effects on cavitation and void growth, *Journal of Materials Science*, 2001, 36, in press

[14] T.F. Guo & L. Cheng, Unstable void growth in plastic IC packaging material, 2001, Mechanics Research, submitted.

[15] A.L. Gurson, Continuum theory in ductile rupture by void nucleation and growth: part I- yield criteria and flow rules for porous ductile media, *Journal of Engineering Materials and Technology*, 1977, 99, 2-15

[16] L. Xia and C.F. Shih, Ductile crack growth – I, a numerical study using computational cells with microstructurally-based length scales, *Journal of Mechanics and Physics of Solids*, 1995, 43, 233-259

[17] H.B. Chew, T.F. Guo & L. Cheng, Modeling interface delamination in plastic IC packages, 2001, *APACK Conference on Advances in Packaging*, Singapore

[18] F.A. Mclintock, a criterion for ductile fracture by growth of holes, *Journal of Applied Mechanics*, 1968, 35, 363-371

[19] J.R.Rice and D.M. Tracey, On the ductile enlargement of voids in triaxial stress fields, *Journal of Mechanics and Physics of Solids*, 1969, 17, 201-217

[20] Y. Huang, J.W. Hutchinson & V. Tvergaard Cavitation instabilities in elastic plastic solids, *Journal of Mechanics and Physics of Solids*, 1991, 39, 223

[21] B.S. Bakhvalov & G.P. Panasenko, *Homogenization: Averaging Processes in Perioidc Media* (1989), Kluwer Academic Publisher

[22] X.J. Fan, Yield criterion at PMMA at a bone-implant interface, *Proceedings of the Fourth China-Japan-USA-Singapore Conference on Biomechanics*, G.T. Yang et al. (eds.), 1995, International Academic Publishers, p360

[23] C.F. Shih, Private communications (2001)

[24] V. Tvergaard and J.W. Hutchinson, The relation between crack growth resistance and fracture process parameters in elastic-plastic solids, , *Journal of Mechanics and Physics of Solids*, 1992, 40, 1377-1397